

Random Occlusion-recovery for Person Re-identification

Di Wu¹, Kun Zhang¹ and De-Shuang Huang^{1*}

¹Institute of Machine Learning and Systems Biology, School of Electronics and Information Engineering, Tongji University, Caoan Road 4800, Shanghai 201804, China

Abstract. As a basic task of multi-camera surveillance system, person re-identification aims to re-identify a query pedestrian observed from non-overlapping cameras or across different time with a single camera. Recently, Deep learning-based person re-identification models have achieved great success in many benchmarks. However, these supervised models require a large amount of labeled image data and the process of manual labeling spends much manpower and time. In this study, we introduce a method to automatically synthesize labeled person images and adopt them to increase the sample number for per identity in datasets. Specifically, we use the block rectangles to occlude the random parts of the persons in the images. Then, a generative adversarial network (GAN) model is proposed to use paired occlusion and original images to synthesize the de-occluded images that similar but not identical to the original images. Afterwards, we annotate the de-occluded images with the same labels of their corresponding raw image and use them to augment the training samples. We use the augmented datasets to train baseline model. The experiment results on CUHK03, Market-1501 and DukeMTMC-reID datasets show that the effectiveness of the proposed method.

Keywords—Generative Adversarial Network, Person Re-identification.

1. Introduction

Person re-identification (ReID) is an important task in many computer vision systems, such as behavioral understanding, threat detection and video surveillance. Given a query person image, it aims to re-identify the same person observed by non-overlapping cameras or across different time with a single camera. The task has drawn significant attention in computer vision community. So far, it is still a challenge issue for the appearance of a person may suffer dramatic change under different camera views. Figure 1 presents several positive pairs from three popular person ReID datasets. Traditional hand-craft methods address the person ReID issue through either finding discriminative feature representations [1-6] or exploiting a suitable distance metric function [7-9]. When the feature representations are obtained, a distance metric function is applied to estimate whether the paired inputs are the same pedestrian or not. Recently, enlightened by the success of deep learning technology, a large amount of literature introduces this technology to address the person ReID and achieves many promising performances. Most of recent state-of-the-art person ReID models are based on deep learning technology. Both the training processes of these models require a large amount of labeled data. However, existing available public datasets are limited in terms of their size and the number of images for per

* Corresponding author. E-mail address: dshuang@tongji.edu.cn.

identity. For example, the average numbers of sample of per identity for these large-scale ReID datasets like CUHK03 [10], Market-1501 [11] and DukeMTMC-ReID [12] are 9.6, 17.2 and 23.5, respectively. Using such scale datasets to train the deep models may lead to over-fitting issue and affect the robustness of them. One way to alleviate this issue is to propose a model that can automatically generate annotated images to increase the sample number for per identity. In this study, we propose a generative adversarial network (GAN)-based framework to generate the labeled images that similar but not identical to the original training images and use the generated images to augment the original training set for person ReID.



Figure 1. Samples of pedestrian images taken from multi-camera views in three datasets. The paired adjacent images are the same pedestrian, from which we can see that the appearance of same pedestrian from different camera views suffer from significantly change.

As shown in Figure 2, firstly, we randomly add block rectangles to the original ReID training images. Secondly, we use the paired occluded images and their ground-truths to train the designed GAN model. Then the trained GAN model is adopted to generate the de-occluded images with the same labels of their corresponding ground-truths. Finally, these generated images are combined with the original ReID training images to feed into the baseline model. We use the proposed model to generate labeled images for two ReID datasets and the augmented datasets to train baseline model to prove the effectiveness of our data augmentation method.

In summary, we make the following contributions:

- (1) We introduce a GAN model that can generate person images which similar but not identical to the original person images;
- (2) We first attempt to assign the original annotation information to the GAN-based generated person images, thus increasing the sample number for per identity;
- (3) We show that the proposed data augmentation method with original annotation information improved the person ReID accuracy on the baseline model.

2. Related work

In this section, we briefly review the existing literature for CNN/LSTM and GANs-based methods for person ReID.

CNN/LSTM Based Person ReID. A large number of deep learning technology-based models are proposed to address the person ReID task. Some of them regard the task as a classification issue. In order to complement the CNN features, Wu et al. [13] propose a fusion feature network (FFN) which can incorporate a variety of hand-crafted features into deep features. Xiao et al. [14] combine multiple datasets to train the CNN model and propose a domain guide dropout strategy to discard worthless neurons for each domain dataset to keep the model in the right track. Lin et al. [15] hold that the person ID recognition learns global representations while attribute classification extracts local aspects (i.e., age, gender, bag and so on). Considering the difference and similarity of the two tasks, they propose combining the attribute classification and identification losses to focus on the local and global aspects of a pedestrian image at the same time. It is worth mentioning that distance metric-based deep models are also frequently adopted in person ReID community. Ding et al. [16] first introduce the triplet model to address the ReID task. Cheng et al. [17] propose an improved triplet loss that can push the different person images farther from each other, and simultaneously pull the same person images closer under the learned deep feature space. Chen et al. [18] introduce a quadruplet loss to enhance the generalization ability of the deep model. There are also exist some literatures adopt LSTM model to learn the spatial information or learn attention-based features for person images. A Siamese LSTM model is proposed by [19] for person ReID. The authors initially divide the image into several rigid parts and extract hand-craft feature like local maximal occurrence and SILTP for each part. Then they use a LSTM model to leverage the contextual information of the local descriptors. Liu et al. [20] propose a LSTM-based attention model that can dynamically produce part attention feature by a recurrent way for localizing the discriminative local regions of the person image.

Data augmentation-based deep model. Recently, some work [12, 21-23] attempt to use the GAN model to extend the scale of person ReID datasets. Zheng et al. [12] first introduce a generative adversarial network (GAN) to generate unlabeled pedestrian samples for ReID datasets. They propose a label smoothing regularization for outliers (LSRO) method to annotate the generated samples. To reduce the domain gap between different datasets, Wei et al. [22] propose a person transfer GAN model which makes up the domain gap via transferring pedestrians in C dataset to D dataset. After transferring the pedestrians from C, the transferred images keep their IDs and hold the similar styles like lightings, backgrounds, etc., with dataset D. Zhong et al. [21] introduce a camera style adaption model to transfer the style of images captured by one camera to another. In [23], the authors introduce a pose-normalization GAN model to alleviate the influence of pose variation. Unlike previous models which assign a new annotation information for the generated samples, we retain the original label information for these generated samples to enlarge the number of image sample for per identity.

3. The proposed method

In this section, we first present the random occlusion method. Then, we illustrate the

architecture of the proposed GAN model. Finally, the loss functions adopted by this model are discussed.

3.1 Random Occlusion.

In the training phase, we add a random occlusion for each training image. As shown in Figure 2, a random rectangle region of the image is selected for erasing by an occlusion. The occlusion can be a black box or a white box with 0, 255 values for its pixels, respectively. In this paper, the values of pixels on R, G and B channels for the occlusion are set to the mean pixel values of R, G and B channels of the ReID dataset, respectively. For example, for the Market-1501 dataset, we set the pixel values on R, G and B channels for the occlusion to 105.3, 99.6 and 97.9, respectively.



Figure 2. The occluded samples

3.2 Network architecture

In this study, the proposed model consists of three major parts, i.e. generator, discriminator and loss function. Similar to the original GAN [23], the network contains two sub-networks: a generator sub-network G and a discriminator sub-network D . While training, we put the paired raw and occluded training images into the generator G . The primary goal of the G network is to synthesize a de-occluded image as close as possible to the raw training image to fool the discriminator D . The sub-network D serves to distinguish the fake de-occluded image generated by G from its corresponding real image. In other words, discriminator D act as a supervisory signal to boost the quality of the synthesized image. Moreover, to further improve the quality of de-occluded image, we introduce the perceptual loss [24] for the G sub-network. In this section, we first discuss the network architecture, then the loss function used in the architecture in detail.

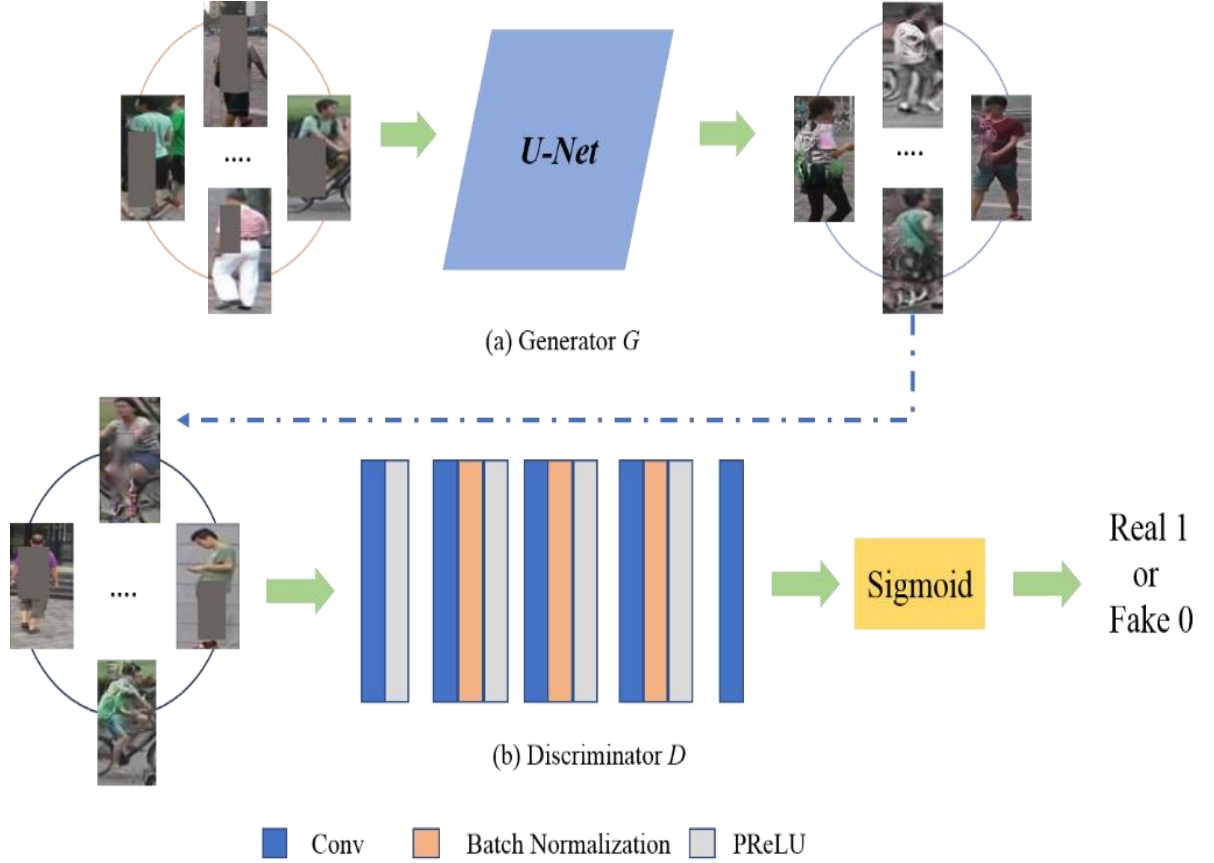


Figure 3. The network architecture

Generative Adversarial Loss. To make the generated image with high quality to fool the discriminator D and to learn a discriminator D with strong ability of discrimination. Given an occluded image I , the optimization objective of GAN network can be written as:

$$\min_G \max_D E_{I \sim P_{data(I)}} [\log(1 - D(I, G(I)))] + E_{I \sim P_{data(I, O)}} [\log D(I, O)] \quad (1)$$

in which O is the output sample, D and G represent the discriminator sub-network and generator sub-network, respectively.

Generator G . The generator sub-network learns a non-linear projection function between the occluded image and its ground truth real image. Through the non-linear projection function, the generator G could generate the de-occluded image that similar but not identical to the original images. In this paper, we use the U-Net as the generator G . It contains a stack of convolutional and de-convolutional layers. The convolutional layers serve as a feature extractor that encodes the basic components of contents for original image while eliminating the occlusion. The de-convolutional decode the encoded contents to restore the content details of raw image. Moreover, several skip connections between the convolutional and de-convolutional are added to preserve more local details.

Generator loss function. Since the generator sub-network tries to generate the de-occluded image that similar but not identical to its corresponding ground truth, therefore, we use the Euclidean loss to train the generator. Given an occluded image I , the function can be

formulated as:

$$L_E(G) = \frac{1}{CMN} \sum_{c=1}^C \sum_{m=1}^M \sum_{n=1}^N \|G(I) - R\|_2^2 \quad (2)$$

in which M, N, C represent the width, height and channels of the images, respectively. R is the ground truth.

In addition to the Euclidean loss, we also use the perceptual loss that can use CNN model to measure the different between the feature representations of ground truth and the outputs of a certain layer of G . The perceptual loss is conducive to improve the quality of the generated images. The loss function can be defined as:

$$L_p(G) = \frac{1}{QWH} \sum_{q=1}^Q \sum_{w=1}^W \sum_{h=1}^H \|VGG_{16}(G(I)) - VGG_{16}(R)\|_2^2 \quad (3)$$

where W, H, Q represent the width, height and channels of a certain high-level layer, respectively. Similar to the work of [24], we use the VGG_{16} model [25] to compute the feature loss.

Discriminator D . For the discriminator D , we use the generated image as negative sample, while using the original image as the positive sample. Then D is designed for classifying whether the input person image is a fake or real. Following the work of [26], we apply a five layers convolutional network that with PReLU and batch normalization operations for the discriminator. After a set of convolutional layers, the sigmoid function is attached to output a probability score. The framework of D is shown in the bottom of Figure 2.

Discriminator loss function. As described above, the discriminator D can be regarded as a binary classification network. Given a mixed image set, the discriminator loss function can be written as:

$$L_D = -\frac{1}{N} \sum_{i=1}^N (U_i \log(D(i)) - (1 - U_i) \log(1 - D(i))) \quad (4)$$

where U_i is the label of I , $U_i=0$ represents i is a fake sample and $U_i=1$ represents i is a real.

4. Experiments and Results

In this section, we present the details of experiments to evaluate the performance of the proposed method. The datasets and training details as well as the comparison results are also discussed.

4.1 Datasets and Evaluation Protocol

We use three well-known person ReID datasets to evaluate the performance of proposed method, including CUHK03 [10], Market-1501 [27] and DukeMTMC-reID [28]. Brief descriptions of three datasets are presented as followings:

CUHK03. The dataset is one of the largest person ReID datasets which contains 13164 images of 1360 identities. All identities are taken from six camera views, and each pedestrian is captured by two cameras. This data set provides two setting. One automatically annotated by a detector and the other manually annotated by human. We use the labeled set to evaluate our model.

Market-1501. This dataset consists of 32643 annotated boxes of 1501 persons. Each pedestrian is collected by at least two cameras and at most six cameras from the front of a supermarket. The boxes of pedestrians are captured by the Deformable Part Model (DPM) detector. The dataset contains 12936 images for training and 19732 images for testing. For this dataset, 12936 images from the training set are used to train the GAN model.

DukeMTMC-reID. The DukeMTMC-reID is created for image-based person ReID. It is a subset of DukeMTMC dataset. It contains 1812 identities with 36411 images. These pedestrian images are captured by eight high-resolution surveillance equipment. Among the 1812 identities, 1404 of them captured by more than two camera views and the rest of them are regarded as distractor identifications.

Evaluation protocols. We use the Cumulative Match Characteristic (CMC) [29] to count the ranks of true matches. The mean Average Precision (mAP) [11] is also adopted. Moreover, we report the re-ranking results based on the *k-reciprocal* encoding [30].

4.2 Implementation details

CNN baselines. We use the CNN baseline proposed by [31]. The DenseNet [32] are used to perform the baseline experiments. The FC layers of them are modified with 1367 and 751 neurons for CUHK03 and Market-1501, respectively. We use the stochastic gradient descent [33] as the optimizer to train the network. The momentum and weight decay are set to 0.9 and $5e-4$, respectively. We set initial learning rate α to 0.01 and decrease it by dividing 0.1 after each 30 epochs. The total training epoch is set to 70.

GAN training details. For the GAN model, we use Pytorch package to implement it. All the occluded and original images are resized into 128×128 pixels. The Adam [34] is used to optimize the network. We set the momentum and initial learning rate to 0.5 and 0.0002, respectively. The network is trained for 150 epochs. When test the GAN model, we randomly regenerate the occluded images and input them to the trained GAN model. Then the generated images with its original label information are used for increasing the sample number for per person. Several generated images from DukeMTMC-reID dataset are shown as Figure 3.



Figure 4. Sample generated de-occluded images from the DukeMTMC-reID dataset, from which we can observe that the de-occluded images are similar but not identical to their corresponding original images.

4.3 Comparison with State-of-the-art

We compare the proposed method with the following approaches: BoW + KISSME [11], SL [35], DNS [36], Gated Siamese [37], Deep Transfer [38], CAN [20], CNN Embedding [39], SVD-Net [40], HydraPlus-Net [41], CNN+DCGAN [12], TriNet [42], CamStyle [43]. The experimental comparison results are shown in this section below.

Evaluation on Market-1501. For the Market-1501, we report both the single-query and multi-query results. The performance on mAP, Rank-1, Rank-5 and Rank-10 of the proposed model are shown in Table 1 and Table 2. From Table 1, we can observe that the proposed method achieves rank-1 accuracy=92.19%, mAP = 78.86% with DensNet, using single query mode. When applying the re-ranking, the results further achieve rank-1 accuracy=93.29%, mAP = 90.36%. Besides, compared to the baseline model, our method increases the rank-1 accuracy and mAP by +2.72%, +5.28 % on single query mode, as well as by +4.98%, +2.42% on multi query mode. Both Table 1 and Table 2 show that the proposed model outperforms the compared methods, which demonstrates the effective of the proposed method.

Table 1. Results (mAP, Rank1, Rank5 and Rank10 matching accuracy in %) on the Market-1501 dataset in the Single-query. 12936 generated images are added to the training set. ‘-’ means no reported result is available.

	Single Query			
Method	mAP	Rank-1	Rank-5	Rank-10
BoW + KISSME [11]	20.76	44.42	-	-
SL [35]	26.35	51.90	-	-
DNS [36]	35.68	61.02	-	-
Gated Siamese [37]	39.55	65.88	-	-
Deep Transfer [38]	65.50	83.70	-	-
CAN [20]	35.90	60.30	-	-
CNN Embedding [39]	59.87	79.51	90.91	-
SVD-Net [40]	62.10	82.3	92.3	95.2
HydraPlus-Net [41]	-	76.9	91.30	94.5
CNN+DCGAN [12]	56.23	78.06	-	-
TriNet [42]+re-rank	81.07	86.67	93.38	-
CamStyle [43]+re-rank	71.55	89.49	-	-
DesNet-Basl	73.58	89.67	96.61	98.16
Ours (DesNet)	78.86	92.19	97.34	98.46
Our (DesNet)+re-rank	90.36	93.29	96.96	97.68

Table 2. Results (mAP, Rank1 and Rank5 matching accuracy in %) on the Market-1501 dataset in the Multi-query. 12936 generated images are added to the training set. ‘-’ means no reported result is available.

	Multi Query		
Method	mAP	Rank-1	Rank-5
BoW + KISSME [11]	19.47	42.64	-
DNS [36]	46.03	71.56	-
Gated Siamese [37]	48.45	76.04	-
Deep Transfer [38]	73.80	89.60	-
CNN Embedding [39]	70.33	85.84	-
CNN+DCGAN [12]	76.10	88.42	-
TriNet [42]+re-rank	87.18	91.75	95.78
DesNet-Basl	79.98	91.84	98.16
Ours (DesNet)	84.96	94.26	97.83

Evaluation on DukeMTMC-reID. As mentioned above, the 1404 pedestrians are chosen for evaluating the proposed method. We use 16522 images of 702 identities to train the GAN and baseline models. The rest of 702 identities are used for testing the baseline model. From Table 3, we can see that our model achieves rank-1 accuracy=82.04%, mAP = 66.81% with the baseline model. The results are further increased to rank-1 accuracy=86.35%, mAP = 82.81% when using the re-ranking tool. Moreover, the method increases the rank-1 accuracy and mAP by +2.72%, +2.68 %, respectively.

Table 3. Results (mAP, Rank1, Rank5 and Rank10 matching accuracy in %) on the DukeMTMC-reID dataset. 16522 generated images are added to the training set. ‘-’ means no reported result is available.

Method	mAP	Rank-1	Rank-5	Rank-10
BoW + KISSME [11]	12.17	25.13	-	-
LOMO+XQDA [44]	17.04	30.75	-	-
CNN+DCGAN [28]	47.13	67.69	-	-
PAN [45]	51.51	71.59	-	-
OIM [46]	47.40	68.10	-	-
CNN embedding [39]	49.30	68.90	-	-
SVD-Net [40]	56.80	76.70	86.4	89.9
TriNet [42]	53.50	72.44	-	-
ACRN [47]	51.96	72.58	84.79	
DesNet-Basl	62.89	79.36	89.73	92.41
Ours (DesNet)	66.81	82.04	91.24	93.89
Ours (DesNet)+re-rank	82.81	86.35	92.87	94.56

Evaluation on CUHK03. On CUHK03 dataset, we use the new protocol proposed by [48], in which 767 pedestrians are used for training and the rest of 700 identities are used for testing. The evaluation procedure of the new protocol is same as Market-1501. Table 4 shows the comparison results of the proposed model against eight existing methods on CUHK03 dataset, including the most recent state-of-the-art approaches. From Table 4, we can see that the proposed model achieves 47.31% mAP accuracy and 50.64% rank-1 accuracy and it increases the rank-1 and mAP baseline accuracies by +5.78% and +5.01%, respectively. Table 4 shows that the proposed model outperforms the compared methods, which further confirms the effectiveness of our proposed method.

Table 4. Results (mAP, Rank1 and Rank5 matching accuracy in %) on the CUHK03 dataset (labeled). ‘-’ means no reported results is available. 7368 generated images are added to the training set Under the new evaluation protocol propose by [48]

Method	mAP	Rank-1	Rank-5
BoW + XQDA [11]	7.29	7.93	-
LOMO+XQDA [44]	13.60	14.80	-
PAN [45] +re-rank	45.80	43.90	56.86
DPFL [49]	40.50	43.00	-
SVD-Net [40]	37.83	40.93	-
HA-CNN [50]	41.00	44.40	-
HCN+re-rank [51]	43.00	40.90	-
MLFN [52]	49.20	54.70	-
DesNet-Basl	42.30	44.86	65.78
Ours(DesNet)	47.31	50.64	70.35
Ours(DesNet)+re-rank	61.95	59.78	70.64

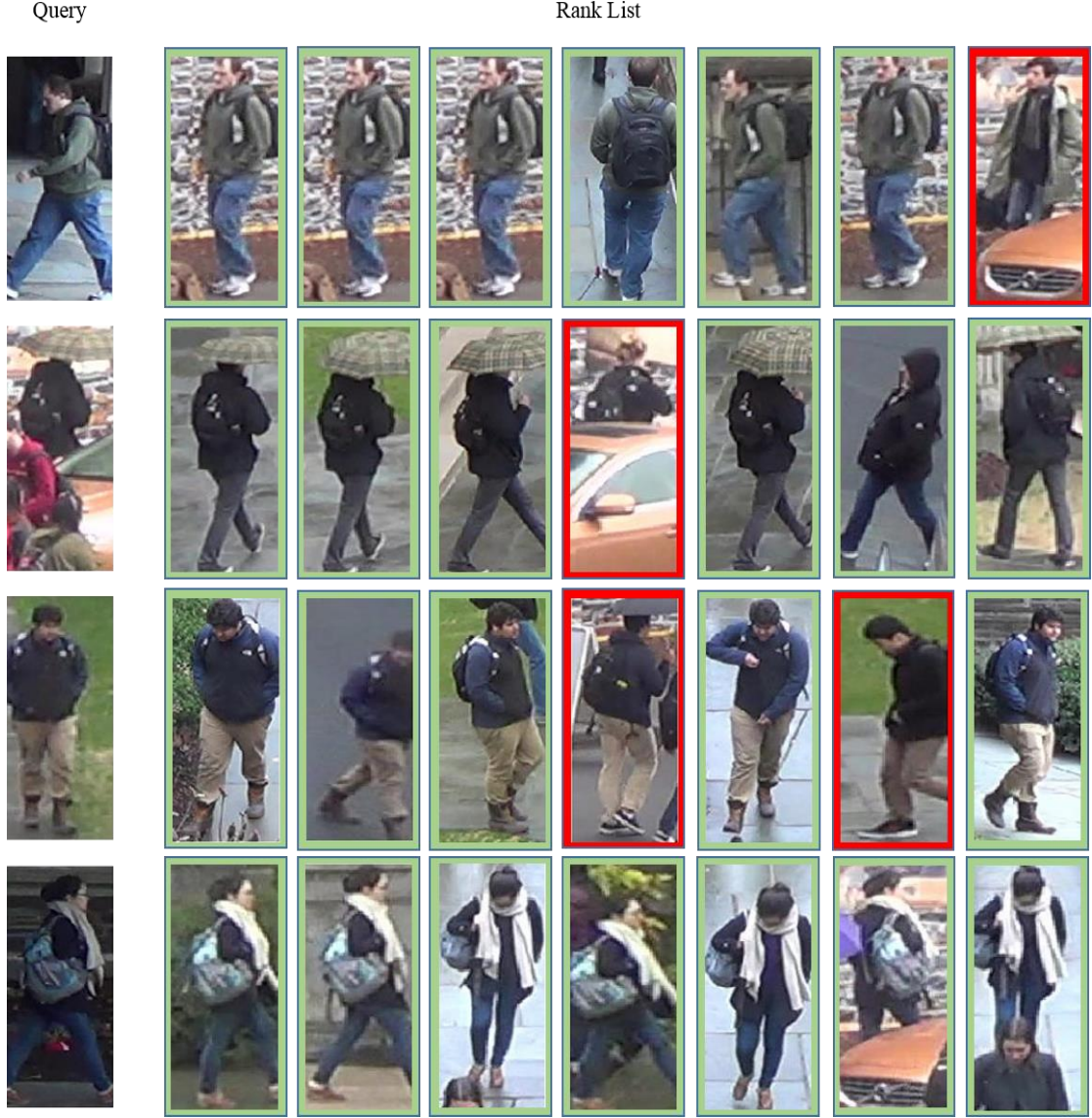


Figure 5. Four example re-identification cases on DukeMTMC-reID dataset. The first column are the query images. The re-identification results are sorted from left to right according to the similarity scores. Images in the green and red boxes indicate true and false retrieval results, respectively.

5. Conclusions

In this study, a data augmentation method based on generative adversarial network (GAN) is proposed for person ReID. Different from the previous GAN-based methods, we retain the original label information for the generated images. In this way, we can increase the sample number for per identity. The original images and the generated images compose of the training set to train the baseline model. We conduct the experiment on three large datasets, i.e. CUHK03, Market-1501 and DukeMTMC-reID with the baseline model. The significant improvement on the three datasets demonstrates the effectiveness of the proposed method.

Acknowledgements

This work was supported by the grants of the National Science Foundation of China, Nos. 61520106006, 31571364, U1611265, 61532008, 61672203, 61402334, 61472282, 61472280, 61472173, 61572447, 61373098 and 61672382, China Postdoctoral Science Foundation Grant, Nos. 2016M601646, and supported by “BAGUI Scholar” Program of Guangxi Province of China. This work has received funding from the European Union’s Horizon 2020 research and innovation programme under the Marie klodowska-Curie grant agreement no. 701697.

References

- [1] D. Gray and H. Tao, "Viewpoint Invariant Pedestrian Recognition with an Ensemble of Localized Features," in *European conference on computer vision*, 2008, pp. 262-275.
- [2] M. Farenzena, L. Bazzani, A. Perina, V. Murino, and M. Cristani, "Person re-identification by symmetry-driven accumulation of local features," in *computer vision and pattern recognition*, 2010, pp. 2360-2367.
- [3] B. Ma, Y. Su, and F. Jurie, "Local descriptors encoded by fisher vectors for person re-identification," in *international conference on computer vision*, 2012, pp. 413-422.
- [4] W. Zheng, S. Gong, and T. Xiang, "Reidentification by Relative Distance Comparison," *IEEE Transactions on Pattern Analysis and Machine Intelligence*, vol. 35, pp. 653-668, 2013.
- [5] B. Macomber, A. B. Probe, R. Woollands, J. Read, J. L. Junkins, B. Macomber, *et al.*, "Enhancements to modified Chebyshev-Picard iteration efficiency for perturbed orbit propagation," *Computer Modeling in Engineering & Sciences*, vol. 111, pp. 567-585, 2015.
- [6] A. B. Younes, "Efficient Orbit Propagation of Orbital Elements Using Modified Chebyshev Picard Iteration Method," in *Special Symposium on Computational Methods in Celestial Mechanics, International Conference on Computational & Experimental Engineering and Sciences*, 2015.
- [7] M. Dikmen, E. Akbas, T. S. Huang, and N. Ahuja, "Pedestrian recognition with a learned metric," in *asian conference on computer vision*, 2010, pp. 501-512.
- [8] Z. Li, S. Chang, F. Liang, T. S. Huang, L. Cao, and J. R. Smith, "Learning Locally-Adaptive Decision Functions for Person Verification," in *computer vision and pattern recognition*, 2013, pp. 3610-3617.
- [9] X. Wang, W. S. Zheng, X. Li, and J. Zhang, "Cross-Scenario Transfer Person Reidentification," *IEEE Transactions on Circuits & Systems for Video Technology*, vol. 26, pp. 1447-1460, 2016.
- [10] W. Li, R. Zhao, T. Xiao, and X. Wang, "DeepReID: Deep Filter Pairing Neural Network for Person Re-identification," in *computer vision and pattern recognition*, 2014, pp. 152-159.
- [11] L. Zheng, L. Shen, L. Tian, S. Wang, J. Wang, and Q. Tian, "Scalable Person Re-identification: A Benchmark," in *IEEE International Conference on Computer Vision*, 2015, pp. 1116-1124.
- [12] Z. Zheng, L. Zheng, and Y. Yang, "Unlabeled Samples Generated by GAN Improve the Person Re-identification Baseline in Vitro," in *IEEE International Conference on Computer Vision*, 2017, pp. 3774-3782.

- [13] S. Wu, Y. C. Chen, X. Li, A. C. Wu, J. J. You, and W. S. Zheng, "An enhanced deep feature representation for person re-identification," in *Applications of Computer Vision*, 2016, pp. 1-8.
- [14] T. Xiao, H. Li, W. Ouyang, and X. Wang, "Learning Deep Feature Representations with Domain Guided Dropout for Person Re-identification," in *Computer Vision and Pattern Recognition*, 2016, pp. 1249-1258.
- [15] Y. Lin, L. Zheng, Z. Zheng, Y. Wu, and Y. Yang, "Improving Person Re-identification by Attribute and Identity Learning," 2017.
- [16] S. Ding, L. Lin, G. Wang, and H. Chao, "Deep feature learning with relative distance comparison for person re-identification," *Pattern Recognition*, vol. 48, pp. 2993-3003, 2015.
- [17] D. Cheng, Y. Gong, S. Zhou, J. Wang, and N. Zheng, "Person Re-identification by Multi-Channel Parts-Based CNN with Improved Triplet Loss Function," in *Computer Vision and Pattern Recognition*, 2016, pp. 1335-1344.
- [18] W. Chen, X. Chen, J. Zhang, and K. Huang, "Beyond Triplet Loss: A Deep Quadruplet Network for Person Re-identification," in *IEEE Conference on Computer Vision and Pattern Recognition*, 2017, pp. 1320-1329.
- [19] R. R. Viorio, B. Shuai, J. Lu, D. Xu, and G. Wang, "A Siamese Long Short-Term Memory Architecture for Human Re-identification," in *European Conference on Computer Vision*, 2016, pp. 135-153.
- [20] H. Liu, J. Feng, M. Qi, J. Jiang, and S. Yan, "End-to-End Comparative Attention Networks for Person Re-identification," *IEEE Transactions on Image Processing A Publication of the IEEE Signal Processing Society*, vol. 26, pp. 3492-3506, 2017.
- [21] Z. Zhong, L. Zheng, Z. Zheng, S. Li, and Y. Yang, "Camera Style Adaptation for Person Re-identification," 2018.
- [22] L. Wei, S. Zhang, W. Gao, and Q. Tian, "Person Transfer GAN to Bridge Domain Gap for Person Re-Identification," *computer vision and pattern recognition*, pp. 79-88, 2018.
- [23] X. Qian, Y. Fu, W. Wang, T. Xiang, Y. Wu, Y. Jiang, *et al.*, "Pose-Normalized Image Generation for Person Re-identification," *arXiv: Computer Vision and Pattern Recognition*, 2017.
- [24] J. Johnson, A. Alahi, and F. F. Li, "Perceptual Losses for Real-Time Style Transfer and Super-Resolution," in *European Conference on Computer Vision*, 2016, pp. 694-711.
- [25] K. Simonyan and A. Zisserman, "Very Deep Convolutional Networks for Large-Scale Image Recognition," *Computer Science*, 2014.
- [26] A. Radford, L. Metz, and S. Chintala, "Unsupervised Representation Learning with Deep Convolutional Generative Adversarial Networks," *Computer Science*, 2015.
- [27] L. Zheng, L. Shen, L. Tian, S. Wang, J. Wang, and Q. Tian, "Scalable Person Re-identification: A Benchmark," in *international conference on computer vision*, 2015, pp. 1116-1124.
- [28] Z. Zheng, L. Zheng, and Y. Yang, "Unlabeled Samples Generated by GAN Improve the Person Re-identification Baseline in Vitro," *international conference on computer vision*, pp. 3774-3782, 2017.
- [29] D. Gray, S. Brennan, and H. Tao, "Evaluating appearance models for recognition, reacquisition, and tracking," 2007.

- [30] Z. Zhong, L. Zheng, D. Cao, and S. Li, "Re-ranking Person Re-identification with k-Reciprocal Encoding," in *IEEE Conference on Computer Vision and Pattern Recognition*, 2017, pp. 3652-3661.
- [31] L. Zheng, Y. Yang, and A. G. Hauptmann, "Person Re-identification: Past, Present and Future," 2016.
- [32] G. Huang, Z. Liu, L. V. D. Maaten, and K. Q. Weinberger, "Densely Connected Convolutional Networks," in *IEEE Conference on Computer Vision and Pattern Recognition*, 2017, pp. 2261-2269.
- [33] L. Bottou, *Stochastic Gradient Descent Tricks*: Springer Berlin Heidelberg, 2012.
- [34] D. P. Kingma and J. Ba, "Adam: A Method for Stochastic Optimization," *Computer Science*, 2014.
- [35] D. Chen, Z. Yuan, B. Chen, and N. Zheng, "Similarity Learning with Spatial Constraints for Person Re-identification," in *IEEE Conference on Computer Vision and Pattern Recognition*, 2016, pp. 1268-1277.
- [36] L. Zhang, T. Xiang, and S. Gong, "Learning a Discriminative Null Space for Person Re-identification," in *Computer Vision and Pattern Recognition*, 2016, pp. 1239-1248.
- [37] R. Rama Varior, M. Haloi, and G. Wang, *Gated Siamese Convolutional Neural Network Architecture for Human Re-Identification*: Springer International Publishing, 2016.
- [38] M. Geng, Y. Wang, T. Xiang, and Y. Tian, "Deep Transfer Learning for Person Re-identification," 2016.
- [39] Z. Zheng, L. Zheng, and Y. Yang, "A Discriminatively Learned CNN Embedding for Person Re-identification," *Acm Transactions on Multimedia Computing Communications & Applications*, vol. 14, 2016.
- [40] Y. Sun, L. Zheng, W. Deng, and S. Wang, "SVDNet for Pedestrian Retrieval," in *IEEE International Conference on Computer Vision*, 2017, pp. 3820-3828.
- [41] X. Liu, H. Zhao, M. Tian, L. Sheng, J. Shao, S. Yi, *et al.*, "HydraPlus-Net: Attentive Deep Features for Pedestrian Analysis," *international conference on computer vision*, pp. 350-359, 2017.
- [42] A. Hermans, L. Beyer, and B. Leibe, "In Defense of the Triplet Loss for Person Re-Identification," *arXiv: Computer Vision and Pattern Recognition*, 2017.
- [43] Z. Zhong, L. Zheng, Z. Zheng, S. Li, and Y. Yang, "Camera Style Adaptation for Person Re-Identification," *computer vision and pattern recognition*, 2018.
- [44] S. Liao, Y. Hu, X. Zhu, and S. Z. Li, "Person re-identification by Local Maximal Occurrence representation and metric learning," *Computer Vision and Pattern Recognition*, pp. 2197-2206, 2015.
- [45] Z. Zheng, L. Zheng, and Y. Yang, "Pedestrian Alignment Network for Large-scale Person Re-identification," *arXiv: Computer Vision and Pattern Recognition*, 2017.
- [46] T. Xiao, S. Li, B. Wang, L. Lin, and X. Wang, "Joint Detection and Identification Feature Learning for Person Search," *computer vision and pattern recognition*, pp. 3376-3385, 2017.
- [47] A. Schumann and R. Stiefelhagen, "Person Re-identification by Deep Learning Attribute-Complementary Information," in *computer vision and pattern recognition*, 2017, pp. 1435-1443.
- [48] Z. Zhong, L. Zheng, D. Cao, and S. Li, "Re-ranking Person Re-identification with k-

- Reciprocal Encoding," *computer vision and pattern recognition*, pp. 3652-3661, 2017.
- [49] Y. Chen, X. Zhu, and S. Gong, "Person Re-identification by Deep Learning Multi-scale Representations," in *international conference on computer vision*, 2017, pp. 2590-2600.
- [50] W. Li, X. Zhu, and S. Gong, "Harmonious Attention Network for Person Re-Identification," *computer vision and pattern recognition*, 2018.
- [51] H. Hsu, C. Chen, H. Tyan, and H. M. Liao, "Hierarchical Cross Network for Person Re-identification," *arXiv: Computer Vision and Pattern Recognition*, 2017.
- [52] X. Chang, T. M. Hospedales, and T. Xiang, "Multi-Level Factorisation Net for Person Re-Identification," *computer vision and pattern recognition*, 2018.